UCRL-JC-128073
PREPRINT

Mechanical Behavior of Ultrahigh Strength, Ultrahigh Carbon Steel Wire and Rod

D. R. Lesuer
C. K. Syn
O. D. Sherby
W. D. Whittenberger

This paper was prepared for submittal to the
Thermomechanical Processing and
Mechanical Properties of Hypereutectoid Steels
TMS Symposium
Indianapolis, IN
September 15-18, 1997

July 22, 1997

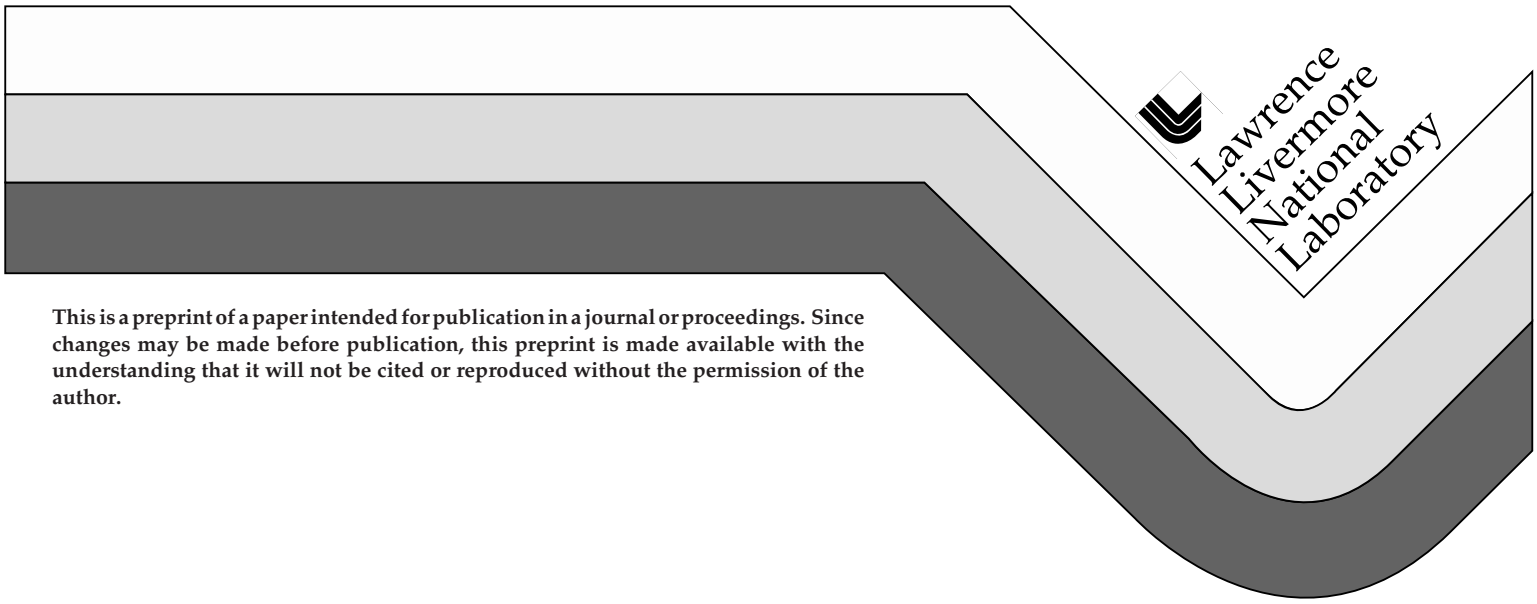

This is a preprint of a paper intended for publication in a journal or proceedings. Since changes may be made before publication, this preprint is made available with the understanding that it will not be cited or reproduced without the permission of the author.

DISCLAIMER

This document was prepared as an account of work sponsored by an agency of the United States Government. Neither the United States Government nor the University of California nor any of their employees, makes any warranty, express or implied, or assumes any legal liability or responsibility for the accuracy, completeness, or usefulness of any information, apparatus, product, or process disclosed, or represents that its use would not infringe privately owned rights. Reference herein to any specific commercial product, process, or service by trade name, trademark, manufacturer, or otherwise, does not necessarily constitute or imply its endorsement, recommendation, or favoring by the United States Government or the University of California. The views and opinions of authors expressed herein do not necessarily state or reflect those of the United States Government or the University of California, and shall not be used for advertising or product endorsement purposes.

MECHANICAL BEHAVIOR OF ULTRAHIGH STRENGTH, ULTRAHIGH CARBON STEEL WIRE AND ROD

Donald R. Lesuer*, Chol K. Syn*, Oleg D. Sherby**,
D.K. Kim*** and W. Daniel Whittenberger****

* Lawrence Livermore National Laboratory, Livermore, CA 94551
** Stanford University, Stanford, CA 94305
*** The Goodyear Tire & Rubber Company, Akron, OH 44309
**** NASA-Lewis Research Center, Cleveland, OH 44135

Abstract

Ultrahigh-carbon steels (UHCSs) can achieve very high strengths in wire or rod form. These high strengths result from the mechanical work introduced during wire and rod processing. These strengths have been observed to increase with carbon content. In wire form, tensile strengths approaching 6000 MPa are predicted for UHCS containing 1.8%C. In this paper, we will discuss the influence of processing (including rapid transformation during wire patenting) and microstructure on the mechanical behavior of UHCS wire. The tensile properties of as-extruded rods are described as a function of extrusion temperature and composition. For spheroidized steels, yield and ultimate tensile strength are a function of grain size, interparticle spacing and particle size. For pearlitic steels, yield and ultimate strength were found to be functions of colony size, carbide size and plate spacing and orientation. Alloying additions (such as C, Cr, Si, Al and Co) can influence the effect of processing on these microstructural features. For spheroidized steels, fracture was found to be a function of the size of coarse carbides and of composition.

Introduction

Many of the papers at this symposium have described the unique mechanical properties that are possible with ultrahigh-carbon steels (UHCSs) and the processing required to achieve them. These properties include superplastic behavior at elevated temperature [1, 2], high strength with good ductility at room temperature [3, 4], and high hardness and high wear resistance [5, 6]. In this paper, we address the processing and resulting microstructures and mechanical properties that can be produced with UHCS in wire or rod form. Specifically, we address the very high strength and good ductility that can be produced in this material when it is subjected to severe plastic deformation during wire drawing or extrusion. The properties produced in these UHCSs can be superior to those found in carbon steels and are important for commercial high strength wire and rod applications including tire cord, bridge cable, wire rope, reinforcing bar, springs and drill rod.

A good example of these improved properties is the ultrahigh strength obtained in high carbon steel wire that is used in tires for automobiles and light trucks. This ultrahigh strength wire is the primary component that defines the structural performance of the tire as well as its weight and rolling resistance. The primary approach for increasing wire strength has been to increase incrementally the carbon content used in high carbon steels for tire cord. Only limited work has been done, however, on steel wire with carbon concentrations much above the eutectoid composition (0.76%C). There are compelling reasons, nevertheless, for studying hypereutectoid steels for high-strength wire applications. The potential for increasing the strength of wires used as tire cord is illustrated in Fig. 1, which shows wire strength as a function of carbon content. The wire diameter (0.28 mm) and the amount of cold work is constant for all data points given as solid circles. The UHCSs are projected to have wire strengths in excess of 4000 MPa. These ultrahigh strength UHCS wires are expected to be significantly stronger than the 3400 MPa wire currently used in premium tires. At 1.8% C, the UHCS wires are projected to have a strength approaching 6000 MPa.

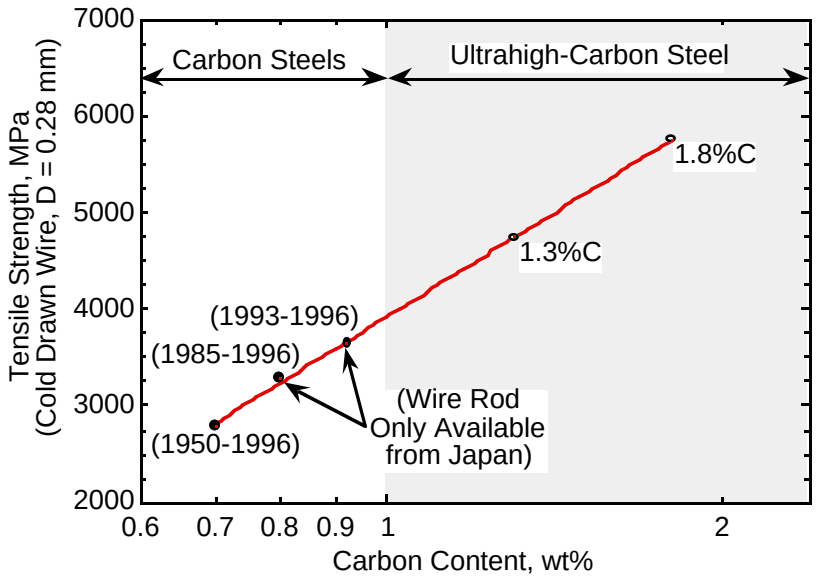

Fig. 1. Influence of carbon content on the strength of cold drawn steel wire. Current premium radial tires use high carbon steel wire with a strength of 3400 MPa. The projected strengths for ultrahigh carbon steels containing 1.3% and 1.8%C are shown in the figure by the open circle symbols.

Processing

General observations

Achieving high strength and good ductility in UHCS requires breaking up the deleterious pro-eutectoid carbide network and developing ultra-fine carbides in spherical or pearlitic form. The formation of this pro-eutectoid carbide network can be influenced by composition, control over phase transformations and thermo-mechanical processing. Ochiai and his co-workers [7-10] have investigated the influence of composition and cooling rate during patenting on the formation of a proeutectoid carbide network. Patenting involves rapid heating to austenite followed by rapid transformation to a fully pearlitic structure. Alloying additions that were found to inhibit the formation of a network include Si and Co. In the cooling rate studies, the tendency to form a proeutectoid carbide network was studied in a 0.2Si-0.5Mn steel as a function of carbon content and cooling rate. The results are shown in Fig. 2. Higher cooling rates tend to suppress the formation of a network. In addition, as the carbon concentration in a hypereutectoid steel is increased, faster cooling rates are required to obtain pearlitic structures without a network. In this study, most of the cooling rates were achieved by lead patenting. The authors concluded that hypereutectoid steels with carbon content up to 1.10% could be patented to obtain a network-free microstructure using commercially-available cooling equipment which can achieve cooling rates of 10-15°C/s.

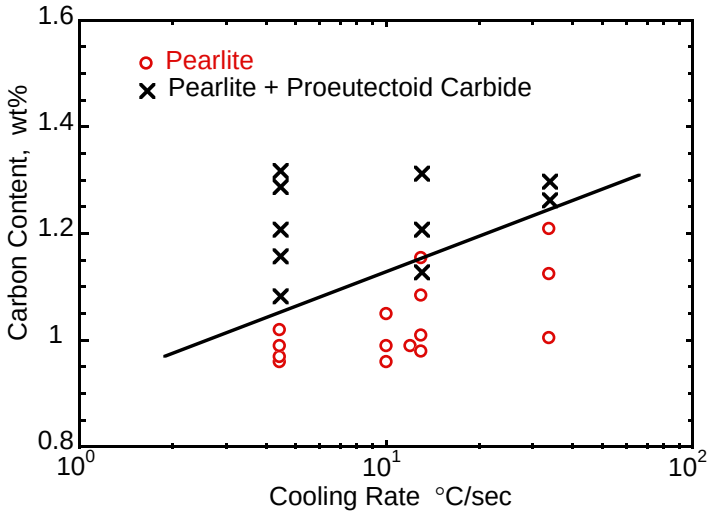

Fig. 2. Effect of cooling rate on the formation of a proeutectoid carbide network in hypereutectoid steels.

Many thermomechanical processing routes have been developed for breaking up the proeutectoid carbide network including hot-and-warm working, warm working, a divorced eutectoid transformation (DET), and a divorced eutectoid transformation with associated deformation (DETWAD) [11-15]. Several papers in this symposium [16-18] describe processing procedures that will achieve this objective. Although such routes have proved successful in achieving desired microstructures and properties in laboratory experiments, they may not be readily amenable to current mass production processing of ultrahigh carbon steels. This is because the mechanical working at low temperatures (700 to 850°C), as required in DETWAD processing, is a drastic change in current production procedures. Recent studies by the authors have shown that network free microstructures can be produced in UHCS by a single-step extrusion process. The extrusion experiments were conducted at the extrusion facility at NASA-Lewis, Cleveland, Ohio. The results of these studies are presented here.

Studies on as-extruded UHCS

Four different composition UHCSs were studied and their compositions are given in Table 1. All four UHCS materials were initially processed to produce a spheroidized microstructure. The

materials were then hot extruded at a high rate in air through a nominal 16:1 reduction ratio using round dies at 900, 1025 and 1150°C. The average strain rate during extrusion was 0.7 s^{-1}. The air cooled as-extruded alloys had microstuctures consisting mainly of pearlite. In general, the true interlamellar spacing of the pearlite (minimum spacing observed) decreased with an increase in the temperature of extrusion. This is probably associated with the larger amount of carbon in solution in austenite prior to transformation with an increase in the austenite extrusion temperature. In addition to pearlite, three other microstructural features are important to note - graphite, carbide networks and spherical carbides. These features were influenced by both the temperature of extrusion and the composition of the steel. At the lowest temperature of extrusion, some graphite was created by the deformation process, typically as fine longitudinal stringers; this limited graphitization was only observed in the chromium-free UHCS materials. At the highest temperature of extrusion, carbide networks at prior austenite grain boundaries were observed in the highest carbon content material (1.8%C). In addition, spherical carbides that remained undissolved at the extrusion temperature (particularly at 900 and 1025°C) remained as spherical carbides during extrusion and subsequent air cooling.

Table 1: Chemical composition of UHCS materials examined in high rate extrusion studies

Designation	Composition
UHCS-119	1.30C, 0.5Si, 0.5Mn, Balance Fe
UHCS-159	1.23C, 1.2Si, 0.5Mn, Balance Fe
UHCS-150	1.15C, 1.6Al, 0.5Mn, Balance Fe
UHCS-180	1.80C, 1.6Al, 0.5Mn, 1.5Cr, Balance Fe.

The influence of composition on the microstructure of UHCS after extrusion at 1150°C is illustrated with the SEM micrographs shown in Fig. 3. The compositions of the alloys are shown below the individual micrographs. The three compositions contain about the same amount of carbon (1.15 to 1.3% carbon), with aluminum or silicon as the principal alloy additions. The three UHCS materials contain no chromium. All compositions show the presence of pearlite. The interlamellar spacing in pearlite is seen to be the smallest in the aluminum containing material (Fig. 3a). With the silicon-containing UHCSs, the interlamellar spacing is seen to increase with an increase in silicon content (Figs. 3b and 3c). Carbide network formation at prior austenite grain boundaries was observed in the aluminum-containing UHCS (Fig 3a), whereas virtually no carbide network was noted in the silicon-containing UHCSs. The aluminum-containing UHCS shows the presence of a discontinuous network of carbides. The obvious conclusion here is that silicon in solution at grain boundaries is more effective than aluminum in inhibiting carbide network formation.

The two potentially detrimental microstructural features developed during the processing of UHCSs are proeutectoid carbide networks and graphite. A thorough, although qualitative, study was made to identify the influenced of extrusion temperature and composition on the formation of these microstructural features. The results are graphically depicted in Fig. 4. Here, the ordinate illustrates the degree of carbide network formation and the abscissa illustrates the degree of graphitization. A number system was used from 1 to 5, with 1 representing the most desired condition (no network and no graphitization). The structural condition for all numbers are described in Fig. 4. Conditions that lead to numbers 1 and 2 were considered to be excellent microstructures, and the shaded area in Fig. 4 reveals that five of the twelve samples reached the

desired condition. These included the 1.8C-1.6 Al UHCS, and the two silicon-containing UHCS materials. The degree of graphitization increased in the order of 1.6% Al, 0.5% Si and 1.2% Si, but only at the lowest temperature of extrusion. Figure 4 also reveals that the degree of carbide network formation increased with the amount of carbon, and with an increase in temperature of extrusion. Silicon appeared to be a more favorable addition for avoiding carbide network formation than aluminum , with the 1.2% Si addition being more favorable than the 0.5% Si. Interestingly, these alloying additions have an opposite effect on graphitization, that is, Al is more effective in inhibiting graphitization than Si.

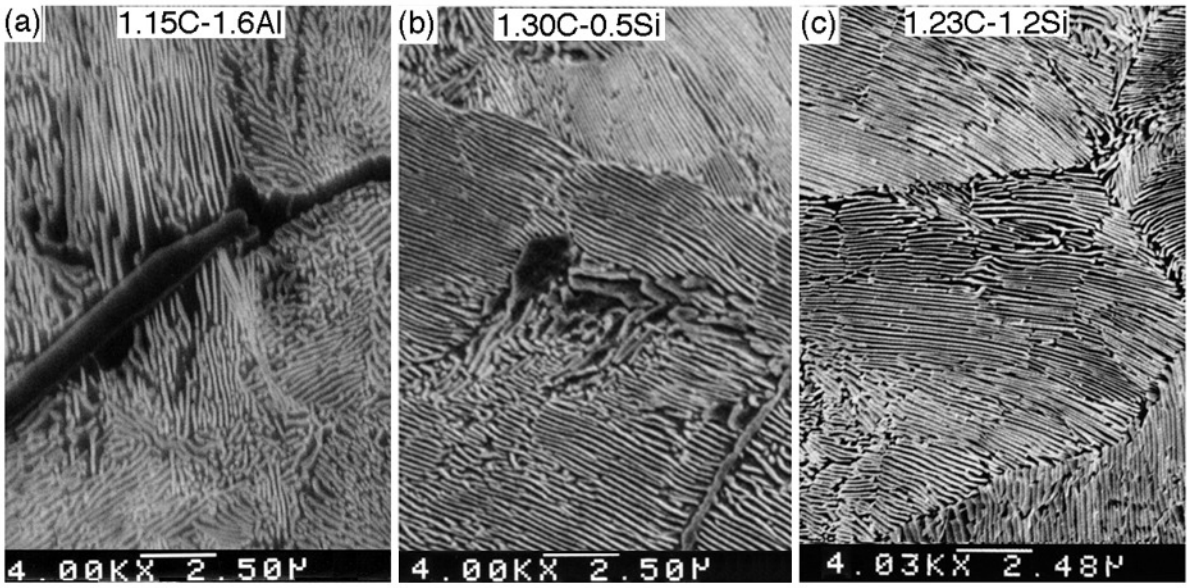

Fig. 3. SEM micrographs showing the influence of composition on the microstructure of UHCS after extrusion at 1150°C.

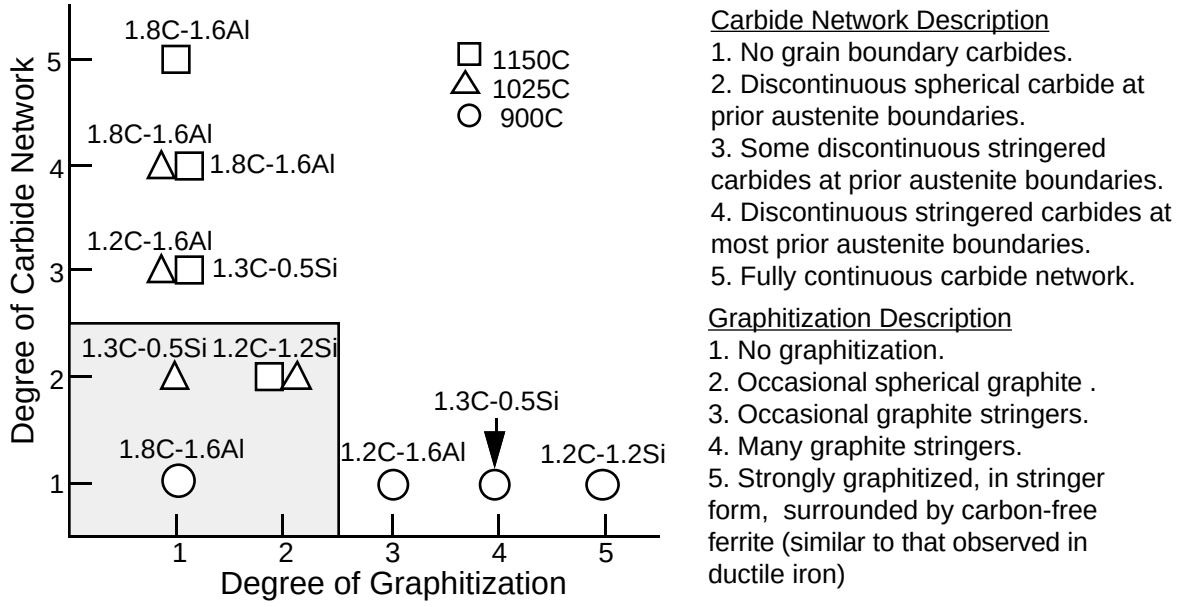

Fig. 4. Graphical depiction of the relative degree of carbide network formation and the degree of graphitization in the four composition UHCSs that were extruded at 900, 1025 and 1100°C.

Strengthening of rod and plates by thermo-mechanical processing

Previous studies of eutectoid and hypereutectoid steels [4, 19] with pearlitic microstructures have shown that the yield strength is derived from hardening contributions associated with pearlite colony size, interlamellar carbide spacing and solute additions. The pearlite colony size and the interlamellar carbide spacing represent the dimensions of microstructural features that impose barriers to dislocation motion. Similarly in a steel with spheroidized microstructures, these microstructural features are ferrite grain size and intercarbide spacing [3]. These strengthening mechanisms contribute to the yield strength in an additive manner and, for eutectoid and hypereutectoid steels, the following equation has been derived

$$\sigma_y = (\sigma_o)_{ss} + 145(D_s^*)^{-1/2} + 460L^{-1/2} \qquad (1)$$

where σ_y is the yield strength, $(\sigma_o)_{ss}$ is the resistance to dislocation motion resulting from solid solution atoms, $(D_s^*)^{-1/2}$ is the carbide spacing (interlamellar spacing or particle spacing) and L is the ferrite grain size or pearlite colony size. The paper by Taleff et al. in this volume [19] provides additional detail into the origins of this equation. The variation of yield strength with $(D_s^*)^{-1/2}$ for two heat treated, pearlitic steels is shown in Fig. 5. As expected, σ_y varies in a linear manner with $(D_s^*)^{-1/2}$. The tensile properties of the as-extruded materials described above were evaluated at room temperature and the yield strengths obtained have been added to the data shown in Fig. 5. As with the heat treated materials shown in Fig. 5, the yield strength of the as-extruded materials varies in a linear manner with $(D_s^*)^{-1/2}$. All UHCSs plotted in Fig. 5 show the same variation of yield strength with interlamellar spacing, i.e., the slopes of the lines in Fig. 5 are equal. The difference between the data sets is the value of the y-intercept, which corresponds to the sum of the strengthening contributions from pearlite colony size and solid solution effects. Based on the analysis discussed by Taleff et al. in reference [4], the Hyzak and Bernstein data [20] has a $(\sigma_o)_{ss}$ value of 60 MPa and the Taleff et al. data has a $(\sigma_o)_{ss}$ value of 330 MPa. These values of $(\sigma_o)_{ss}$ are close to the intercept values at infinite pearlite spacing in Fig. 5. Thus, for the steels studied, significantly more strengthening is derived from solid solution effects that the resistance to dislocation motion imposed by pearlite colony boundaries. The as-extruded data in Fig. 5 suggests that the increase in strength from solid solution strengthening with Si is less than but comparable to the increase in strength from Al.

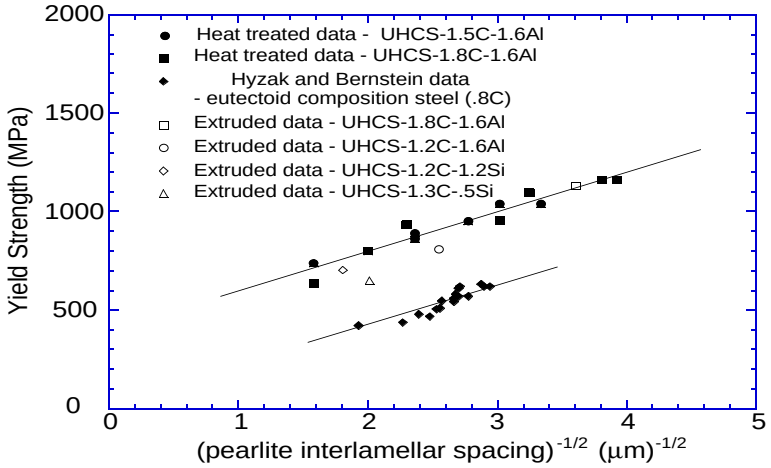

Fig. 5. Yield strength versus inverse square root of the pearlite interlamellar spacing for the four, as-extruded UHCSs. Data is also provided for two heat treated UHCSs and the data of Hyzak and Bernstein for a eutectoid composition steel.

Strengthening of wires by severe cold drawing

A number of investigators have studied the increase in strength that results from cold drawing of eutectoid and hypereutectoid steel wires [8, 21-25]. Most of these studies have reported strength as a function of wire diameter. Data from seven such materials are shown in Fig. 6. Five of these materials are hypereutectoid composition wires and two of the materials are eutectoid composition wire (piano wire and the data of Kim and Shemenski). The starting strength in all these studies is derived from a fully pearlitic microstructure produced as a result of a patenting treatment. The strengthening produced by these microstructures represents an important starting point for the very high strengths typically observed in severely drawn wire. The influence of cold wire drawing on the strength of hypereutectoid steels can be understood through further analysis of the data in Fig. 6. The increase in strength resulting from cold wire drawing was calculated as a function of drawing strain by subtracting the strength of the wire in the cold-drawn condition from the strength in the patented condition. Results are shown in Fig. 7 for three hypereutectoid steels with similar compositions. These materials had different as-patented strengths and different starting diameters. The results fall on a common curve suggesting that a common mechanism is responsible for the increase in strength by wire drawing.

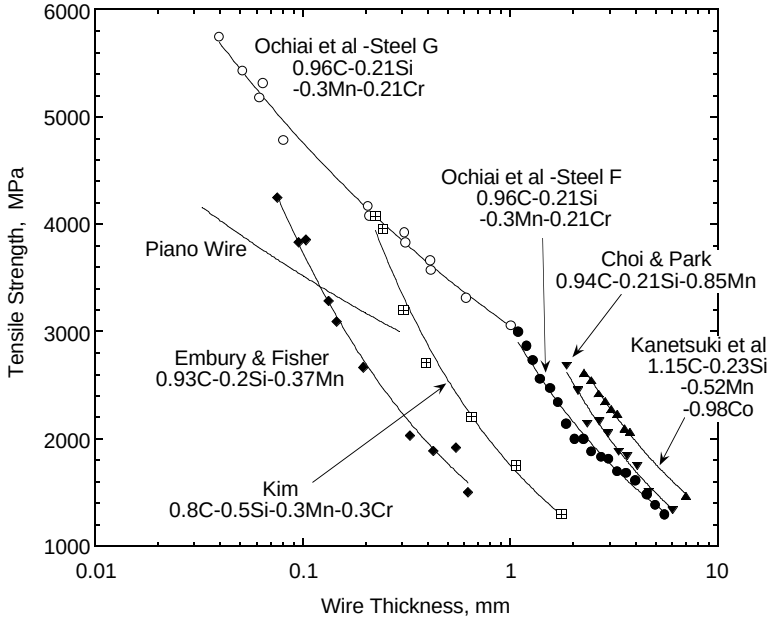

Fig. 6. Tensile strength as a function of wire diameter during wire drawing for eutectoid and hypereutectoid steels.

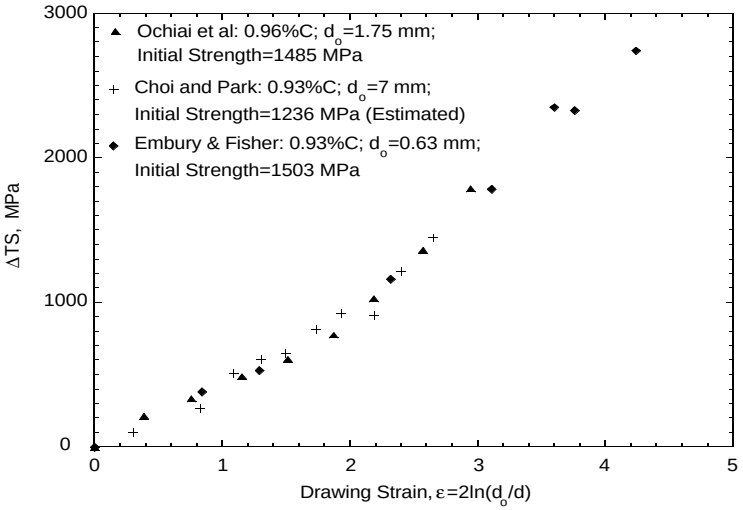

Fig. 7. Strength increment as a function of wire drawing strain in hypereutectoid steels with similar composition

.

Embury and Fisher [23] have studied microstructure development during cold drawing of a Fe-.93C-.2Si-.37Mn wire and have established the principal strengthening mechanisms. Immediately after patenting the pearlitic colonies had randomly oriented plates. Drawing produced considerable alignment of these pearlite plates and numerous fractured pearlite plates were observed. In addition, dislocation cells developed between the carbide plates during wire drawing. With increasing drawing strain, these cells in the ferrite elongated and their size normal to the axis of wire drawing (λ) decreased. The yield strength of the wire was found to vary with λ according to a Hall-Petch like equation given as

$$\sigma_y = \sigma_o + k_y \lambda^{-1/2} \qquad (2)$$

where σ_y is the yield strength, σ_o is the strength from all sources other than dislocation cells, and k_y is a constant. The strengthening in these severely drawn wires with stable sub-structures resulted from the cell walls acting as barriers to dislocation motion.

The evolution of the dislocation substructure during cold drawing and the contribution of a stable cellular structure to strengthening have been studied by Langford and Cohen [26] for pure iron. In contrast to the work of Embury and Fisher, the yield strength was found to vary as an inverse linear function of the dislocation cell size (λ^{-1}). The dependence of flow stress on λ^{-1} was theorized to result from the work of deformation required to generate the length of dislocation line necessary to produce the imposed deformation. A comparison of the Embury and Fisher data on a Fe-.93C steel (which showed that strength varied as $\lambda^{-1/2}$) and the Langford and Cohen data on pure iron (which showed that strength varied as λ^{-1}) is shown in Fig. 8. Clearly different slopes are appropriate for the two data sets, although there is an overall continuity in the data for the two investigations. It is important to note, however, that, in addition to the Fe-.93C alloy, Embury and Fisher also studied a commercially pure iron (Ferrovac E) and found that the yield strength varied as $\lambda^{-1/2}$. Thus for pure iron there is a discrepancy between the experimental data of Embury and Fisher, who observed that the yield strength varied as $\lambda^{-1/2}$, and the data of Langford and Cohen who observed that the yield strength varied as λ^{-1}. Additional work is needed to explain the difference between these two experimental findings.

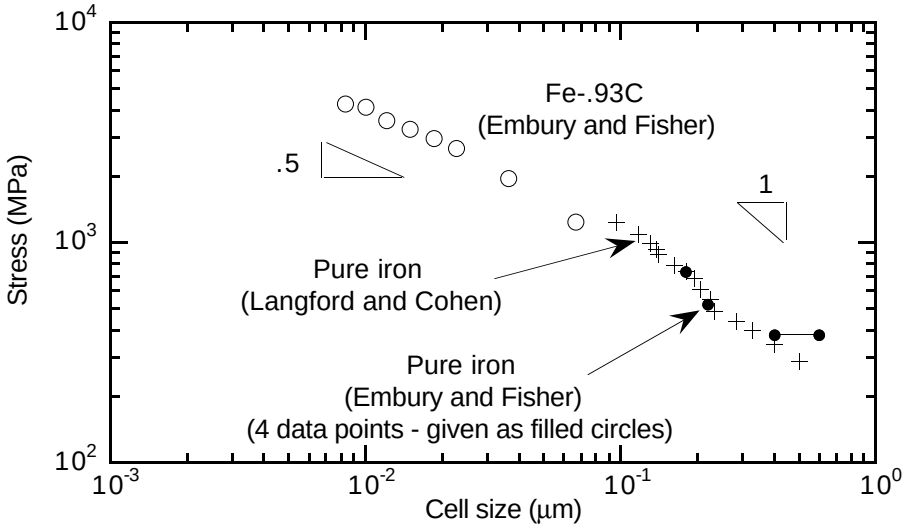

Fig. 8. Stress versus cell size for drawn Fe-.93C (data of Embury and Fisher) and pure iron. The pure iron data is from the two investigations (Embury and Fisher and Langford and Cohen).

Two observations relative to the strength levels shown in Fig. 8 are relevant to the various mechanisms of strengthening. First, the initial (as heat treated) strength before wire drawing is higher in the hypereutectoid steel than in pure iron. Clearly this difference arises from the strengthening effects of the carbide plates in the pearlitic steel. By analogy with the experimental work of Taleff et al., one might expect that the strength of a pearlitic steel results from the sum of strengthening contributions from different barriers to dislocation motion. Thus, for a severely worked pearlitic steel,

$$\sigma_y = (\sigma_o)_{ss} + \sigma_{pearlite} + \sigma_{colony} + \sigma_{cell} \qquad (3)$$

where $(\sigma_o)_{ss}$, $\sigma_{pearlite}$, σ_{colony} and σ_{cell} represent the resistance to dislocation motion resulting from solid solution addditions ($(\sigma_o)_{ss}$), pearlitic plate spacing ($\sigma_{pearlite}$), pearlite colony size (σ_{colony}) and dislocation cell size (σ_{cell}). The$(\sigma_o)_{ss}$, $\sigma_{pearlite}$, σ_{colony} terms for hypereutectoid steels are given in equation (1). The σ_{cell} term is shown as a function of drawing strain in Fig. 7 (assuming in a severely drawn wire that the yield strength equals the tensile strength). The data in Fig. 7 suggests that for severely drawn wire the cell size dominates the strength of the wire, and the pearlite spacing and pearlite colony size are secondary contributors. Furthermore, this view agrees with the continuous nature of the data shown in Fig. 7, which compares a pearlitic structure wire with a totally ferritic structure wire. The σ_{cell} data in Fig. 7 is for a single composition hypereutectoid steel. It is informative to examine the strength increment due to drawing for all the steels shown in Fig. 6. The results are shown in Fig. 9, which shows a good correlation between the incremental increase in strength and the drawing strain. There is some scatter in the data; the general trend, however, is that steels with higher carbon content have higher strength increments for a given amount of drawing strain.

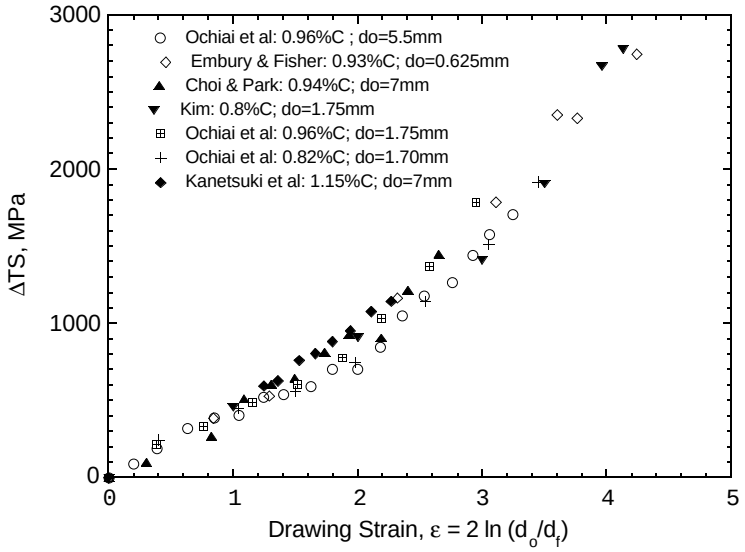

Fig. 9. Strength increment as a function of wire drawing strain for the eutectoid and hypereutectoid steels shown in Fig. 6.

The second observation that can influence the strength levels in Figs. 6 and 8 is the size of the initial cells that form. As noted by Embury and Fisher, who compared dislocation substructures produced in commercially pure iron and Fe-.93C (with both coarse and fine pearlite), the presence of carbide plates produced a smaller initial cell size in the ferrite. In addition, reducing the interlamellar spacing, reduced the initial cell size. Thus, by analogy, increasing the carbon content for a given platelet size will reduce the interlamellar spacing and thus the initial cell size.

Comparison with other high strength fibers

The wire strengths described here (e.g., the 5000 MPa wire strength shown in Fig. 1) represents a very high value - exceeding 20% of the theoretical cohesive strength of steel. Figure 10 compares the strength of these highly drawn UHCS wires with the strength of bulk materials as well as other fibers that are used as reinforcement in composite materials. The highly drawn UHCS wires are significantly stronger than bulk metals used in structural applications but more importantly the strength of these wires compares favorably with those of other reinforcing fibers such as S-glass, Kevlar-49 and carbon fiber. The figure also shows the cost of the reinforcing fibers; UHCS wire (with an estimated as-processed cost of $.60/pound) is significantly less expensive than other reinforcing fibers. Thus one can expect significant commercial applications with the ultrahigh strength hypereutectoid steel wires described here.

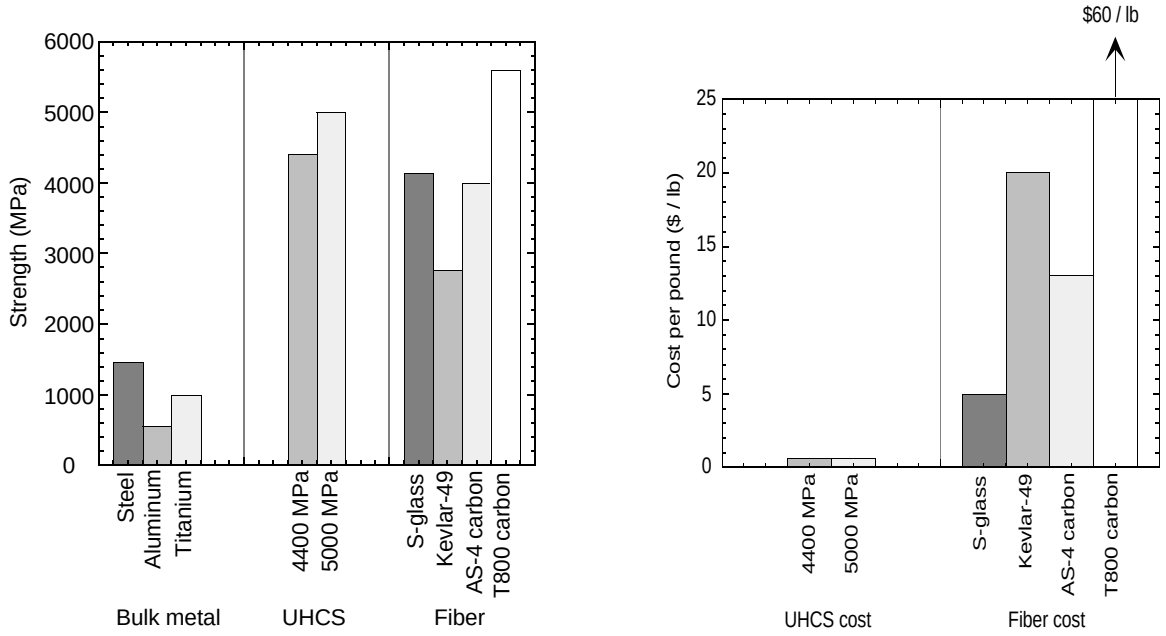

Fig. 10. Comparisons of strength and cost of UHCS wire with other bulk structural metals and reinforcing fibers used in composite materials

Fracture

Previous work has established that the strength of high carbon and ultrahigh carbon steels is limited by the fracture strength of the carbides. Suppressing fracture is necessary to obtain the very high strengths projected in Fig. 1 for UHCS. Work by Lesuer, Syn and Sherby [27] has established the influence of composition and microstructure on the fracture strength of the carbides. SEM and TEM studies showed that failure in a spheroidized UHCS-1.8%C material initiates through tensile separation of carbide-carbide boundaries in the coarse carbide particles. An example of a carbide particle that was fractured into two parts is shown in the TEM photomicrograph presented in Fig. 11. Fracture is clearly at a grain boundary because both ends of the crack meet at obvious triple points. Diffraction patterns identified that a large misorientation existed between the two separated carbide grains. It was concluded that failure in spheroidized hyper-eutectoid steels is the result of a crack-nucleation dominated process which is dependent on a critical fracture stress. The fracture strength for UHCS was shown to vary as the inverse square root of the average coarse carbide particle size. The results indicate that fracture

of the composite occurs when a critical stress is reached which is solely a function of the average coarse spheroidized carbide particle size (typically found at ferrite matrix grain boundaries).

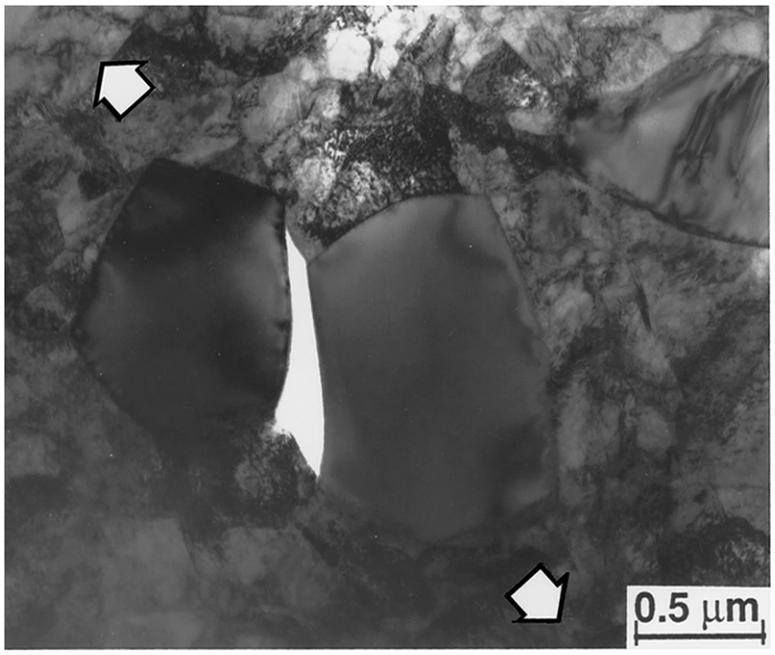

Fig. 11. TEM of a large carbide particle fractured in a UHCS-1.8% during tensile testing. Tensile axis is indicated with arrows.

Another important variable influencing the fracture strength of spheroidized hypereutectoid steels is the intrinsic fracture strength of the carbide. In detailed analyses of fracture data for various hypereutectoid steels, Lesuer, Syn and Sherby [27] developed a fracture model based on the concept that the ferrite matrix applies stress to the carbide particle and thus the stress in the ferrite matrix is the driving force for crack initiation at the grain boundaries within the coarse carbides. The authors calculated the ferrite matrix fracture stress by averaging the ferrite stress using upper and lower bound concepts. In order to fulfill the fracture mechanics requirement that the ferrite matrix fracture strength must be zero at infinite carbide (crack) size, Lesuer et al. made the discovery that the strength of the carbide was a function of composition of the hypereutectoid steels studied. This discovery is graphically illustrated in Fig. 12 where three groups are shown according to composition differences. The unalloyed and low alloyed hypereutectoid steels show higher values of carbide strength than the more extensively alloyed steels. It would appear that elements that dissolve in the carbide decrease the grain boundary strength. Thus, it is postulated that chromium and aluminum, which dissolve in iron carbide and distort the carbide lattice (or form carbide of a different structure), decrease the grain boundary carbide strength. On the other hand, silicon, which does not dissolve in the carbide, does not influence the grain boundary carbide strength (material of Le Roy et al. [28]). Manganese is known to produce an M_3C type carbide, as does iron, and therefore may behave in a indistinguishable way from iron in influencing the grain boundary strength.

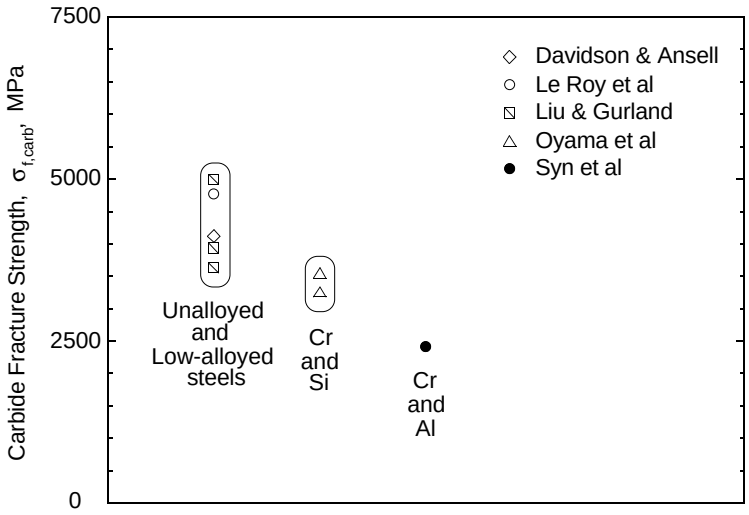

Fig. 12. Predicted carbide fracture strength as a function of composition for spheroidized hypereutectoid steels.

Summary and Concluding Remarks

This paper has reviewed the processing required to obtain high strength as well as the resulting properties and strengthening mechanisms in wire and rod material. Important conclusions are as follows.

- Very high strengths are possible in hypereutectoid steel wire or rod. At 1.8% C, hypereutectoid steel wires are projected to have a strength approaching 6000 MPa.
- Achieving high strength requires eliminating the continuous carbide network that can form during cooling from temperatures in the austenite phase field. In addition, graphitization should be minimized or eliminated. The network can be broken up by thermo-mechanical processing or suppressed from forming by alloying additions (such as Si or Co) or transformation control using suitable cooling rates. Similarly, graphitization can be controlled by composition and processing.
- Studies on as-extruded UHCS have shown that the degree of carbide network formation increased with the amount of carbon, and with an increase in temperature of extrusion. Silicon appears to be a more favorable addition for avoiding carbide network formation than aluminum. For a 1.8C-1.6 Al UHCS, and two silicon-containing UHCS materials extruded at 900°C, the degree of graphitization increased in the order of 1.6% Al, 0.5% Si and 1.2% Si.
- The yield strength in hypereutectoid steels has been shown to result from additive strengthening contributions from solid solution additions, pearlite spacing, pearlite colony size and dislocation cell size. For severely drawn wire, the strengthening due to dislocation cells can dominate the strength of the wire.
- Fracture was found to initiate through tensile separation of carbide-carbide boundaries in coarse carbide particles. The fracture strength is a function of the size of coarse carbides and of composition.

Acknowledgments

This work was performed under the auspices of the U. S. Department of Energy by Lawrence Livermore National Laboratory under contract No. W-7405-ENG-48. Support was provided by the Laboratory Directed Research and Development Program.

References

1. O. D. Sherby, B. Walser, C. M. Young, and E. M. Cady, "Superplastic UHCSs," Scripta Metallurgica, 9 (1975), 569-574.
2. B. Walser and O. D. Sherby, "Mechanical Behavior of Superplastic UHCSs at Elevated Temperature," Metallurgical Transactions A, 10A (1979), 381-386.
3. C. K. Syn, D. R. Lesuer, and O. D. Sherby, "Influence of Microstructure on the Tensile Prop. of Spheroidized UHCS," Metallurgical Transactions A, 25A (July) (1994), 1481-1493.
4. E. M. Taleff, C. K. Syn, D. R. Lesuer, and O. D. Sherby, "Pearlite in Ultrahigh Carbon Steels: Heat Treatments and Mechanical Properties," Metallurgical Transactions A, 27A (1996), 111-120.
5. R. K. Steele, "Railroad Rails and Switching Frogs: Applications for Hypereutectoid Steels," in *Thermomechanical Processing and Mechanical Properties of Hypereutectoid Steels and Cast Irons*, D. R. Lesuer, C. K. Syn, and O. D. Sherby, Eds., this volume.
6. M. Ueda, "Application of Hypereutectoid Steel for Rails in Heavy Tracks," in *Thermomechanical Processing and Mechanical Properties of Hypereutectoid Steels and Cast Irons*, D. R. Lesuer, C. K. Syn, and O. D. Sherby, Eds., this volume.
7. I. Ochiai, H. Ohba, Y. Yohji, and M. Nagumo, "Effect of Central Segregation on Drawability of High Carbon Steel Wire Rod Manufactured from Continuously Cast Blooms," Tetsu-to-Hagane (Journal of the Iron and Steel Institute of Japan), 74 (1988), 1625-1632.
8. I. Ochiai, S. Nishida, H. Ohba, and A. Kawana, "Application of Hypereutectoid Steel for Development of High Strength Steel Wire," Tetsu-to-Hagane (Journal of the Iron and Steel Institute of Japan), 79 (1993), 89-95.
9. I. Ochiai, S. Nishida, and H. Tashiro, "Effects of Metallurgical Factors on Strengthening of Steel Tire Cord," Wire Journal International, 26 (1993), 50-61.
10. I. Ochiai, S. Nishida, H. Ohba, O. Serikawa, and H. Takahashi, "Development of Ultra-High Strength Hypereutectoid Steel Wires," Material Japan (Bulletin of the Japan Institute of Metals), 33 (1994), 444-446.
11. O. D. Sherby, T. Oyama, D. W. Kum, B. Walser, and J. Wadsworth, "UHCSs (JOM)," Journal of Metals (JOM), 37 (1985), 50-56.
12. T. Oyama, O. D. Sherby, J. Wadsworth, and B. Walser, "Application of the Divorced Eutectoid Transformation to the Development of Fine-Grained, Spheroidized Structures in UHCSs," Scripta Metallurgica, 18 (1984), 799-804.
13. T. Oyama, O. D. Sherby, and J. Wadsworth, "DET Process and Product of UHCSs," U. S. Patent No. 4,448613 (1984).
14. O. D. Sherby and T. Oyama, "UHCS Alloy and Processing Thereof," U. S. Patent No. 4,533,390 (1985).
15. W. B. Avery, "The Influence of Heat Treatment on the Microstructure and Properties of Fine-Grained UHCSs," M.S. Dissertation Stanford University (1982).

16. J. Wadsworth and O. D. Sherby, "The History of Ultrahigh Carbon Steels," in *Thermomechanical Processing and Mechanical Properties of Hypereutectoid Steels and Cast Irons*, D. R. Lesuer, C. K. Syn, and O. D. Sherby, Eds., this volume.
17. B. Walser, T. Oyama, U. Ritter, and O. D. Sherby, "Microstructures and Mechanical Properties of an Ultrahigh Carbon Steel Procesed by the Divorced Eutectoid Transformation," in *Thermomechanical Processing and Mechanical Properties of Hypereutectoid Steels and Cast Irons*, D. R. Lesuer, C. K. Syn, and O. D. Sherby, Eds., this volume.
18. O. A. Ruano, M. Carci, J. Ibanez, C. Bertrand, F. Penalba, and O. D. Sherby, "Ultrahigh Carbon Steel and Ductile Iron Research in Spain," in *Thermomechanical Processing and Mechanical Properties of Hypereutectoid Steels and Cast Irons*, D. R. Lesuer, C. K. Syn, and O. D. Sherby, Eds., this volume.
19. E. M. Taleff, C. K. Syn, D. R. Lesuer, and O. D. Sherby, "A Comparison of Mechanical Behavior in Pearlitic and Spheroidized Hypereutectoid Steels," in *Thermomechanical Processing and Mechanical Properties of Hypereutectoid Steels and Cast Irons*, D. R. Lesuer, C. K. Syn, and O. D. Sherby, Eds., this volume.
20. J. M. Hyzak and I. M. Bernstein, "The Role of Microstructure on the Strength and Toughness of Fully Pearlitic Steels," Metallurgical Transactions A, 7A (1976), 1217-1224.
21. D. R. Lesuer, C. K. Syn, O. D. Sherby, and D. K. Kim, "Processing and Mechanical Behavior of Hypereutectoid Steel Wire," in *Metallurgy, Processing and Applications of Metal Wires*, H. G. Paris and D. K. Kim, Eds. Warrendale, PA: TMS, (1996), 109-121.
22. Y. Kanetsuki, N. Ibaraki, and S. Ashida, "Effect of Cobalt Addition on Transformation Behavior and Drawability of Hypereutectoid Steel Wire," Iron and Steel Institute of Japan International, 31 (1991), 304-311.
23. J. D. Embury and R. M. Fisher, "The Structure and Properties of Drawn Pearlite," Acta Metallurgica, 14 (1966), 147-159.
24. D. K. Kim and R. M. Shemenski, US Patent No. 5,167,727, (1992).
25. H. C. Choi and K. T. Park, "The Effect of Carbon Content on the Hall-Petch Parameters in the Cold-Drawn Hypereutectoid Steels," Scripta Materialia, 34 (1996), 857-862.
26. G. Langford and M. Cohen, "Strain Hardening of Iron by Severe Plastic Deformation," Transactions ASM, 62 (1969), 623-638.
27. D. R. Lesuer, C. K. Syn, and O. D. Sherby, "Fracture Behavior of Spheroidized Hypereutectoid Steels," Acta Metallurgica et Materialia, 43 (1995), 3827-3835.
28. G. LeRoy, J. D. Embury, G. Edward, and M. F. Ashby, "A Model of Ductile Fracture Based on the Nucleation and Growth of Voids," Acta Metallurgica, 29 (1981), 1509-1522.

Technical Information Department • **Lawrence Livermore National Laboratory**
University of California • Livermore, California 94551